Fenton, G. A., Griffiths, D. V. & Williams, M. B. (2005). *Géotechnique* **55**, No. 1, 55–62

Reliability of traditional retaining wall design

G. A. FENTON*, D. V. GRIFFITHS† and M. B. WILLIAMS‡

Retaining wall design has long been carried out with the aid of either the Rankine or Coulomb theories of earth pressure. To obtain a closed-form solution, these traditional earth pressure theories assume that the soil is uniform. The fact that soils are actually spatially variable leads, however, to two potential problems in design: do sampled soil properties adequately reflect the effective properties of the entire retained soil mass, and does spatial variability of soil properties lead to active earth pressure effects that are significantly different from those predicted using traditional models? This paper combines non-linear finite element analysis with random field simulation to investigate these two questions and assess just how safe current design practice is. The specific case investigated is a two-dimensional frictionless wall retaining a cohesionless drained backfill. The wall is designed against sliding using Rankine's earth pressure theory. The design friction angle and unit weight values are obtained by sampling the simulated random soil field at one location, and these sampled soil properties are then used as the effective soil properties in the Rankine model. Failure is defined as occurring when the Rankine predicted force acting on the retaining wall, modified by an appropriate factor of safety, is less than that computed by the random finite element method employing the actual soil property (random) fields. Using Monte Carlo simulation, the probability of failure of the traditional design approach is assessed as a function of the factor of safety used and the spatial variability of the soil.

KEYWORDS: earth pressure; retaining walls; statistical analysis

La conception des murs de soutènement se fait depuis longtemps à l'aide de la théorie de Rankine ou de la théorie de Coulomb sur la pression terrestre. Pour obtenir une solution en forme fermée, ces théories de pression terrestre traditionnelles présument que le sol est uniforme. Cependant, le fait que les sols sont en fait variables dans l'espace mène à deux problèmes de conception potentiels : est-ce que les propriétés du sol échantillonné représentent de manière adéquate les propriétés effectives de toute la masse de sol retenue et est-ce que la variabilité spatiale des propriétés du sol mène à des effets actifs de pression terrestre qui sont largement différents de ceux prédits en utilisant les modèles traditionnels ? Cet exposé combine des analyses d'éléments finis non linéaires à des simulations aléatoires sur le terrain pour étudier ces deux questions et évaluer le degré de fiabilité de la pratique de design courante. Le cas spécifique examiné ici est un mur sans friction en deux dimensions retenant un remblai drainé sans cohésion. Le mur a été conçu contre le glissement en utilisant la théorie de pression terrestre de Rankine. L'angle de friction nominal et les valeurs de poids unitaire sont obtenues en faisant des échantillons du champs aléatoire simulé en un endroit ; les propriétés échantillonnées sont alors utilisées comme les propriétés effectives du sol dans le modèle de Rankine. La défaillance est définie comme se produisant lorsque la force prévue de Rankine agissant sur le mur de soutènement et modifiée par un facteur de sécurité approprié est inférieure à celle calculée par la méthode d'éléments finis aléatoires employant les champs (aléatoires) de propriété du sol réel. En utilisant une simulation de Monte Carlo, la probabilité de défaillance de la méthode de conception traditionnelle est évaluée comme fonction du facteur de sécurité utilisé et de la variabilité spatiale du sol.

INTRODUCTION

Retaining walls are, in most cases, designed to resist active earth pressures. The forces acting on the wall are typically determined using the Rankine or Coulomb theories of earth pressure after the retained soil properties have been estimated. This paper compares the earth pressures predicted by Rankine's theory with those obtained via finite element analysis in which the soil is assumed to be spatially random. The specific case of a two-dimensional cohesionless drained soil mass with a horizontal upper surface retained by a vertical frictionless wall is examined. For a cohesionless soil the property of interest is the friction angle. The wall is assumed to be able to move away from the soil a sufficient distance to mobilise the frictional resistance of the soil.

The traditional theories of lateral active earth pressures are derived from equations of limit equilibrium along a planar surface passing through the soil mass. The soil is assumed to have a spatially constant friction angle. Under these conditions, and for the retaining problem considered herein, Rankine proposed the active earth pressure coefficient to be

$$K_a = \tan^2\left(45 - \frac{\phi'}{2}\right) \quad (1)$$

where ϕ' is the soil's drained friction angle. Traditional theories assume that the unit weight, γ, is spatially constant also, so that the total lateral active earth force acting on a wall of height H, at height $H/3$, is given by

$$P_a = \tfrac{1}{2}\gamma H^2 K_a \quad (2)$$

The calculation of the lateral design load on a retaining wall involves estimating the friction angle, ϕ', and the unit weight, γ, and then using equations (1) and (2). To allow

Manuscript received 29 April 2004; revised manuscript accepted 19 October 2004.
Discussion on this paper closes on 1 August 2005, for further details see p. ii.

* Department of Engineering Mathematics, Dalhousie University, Halifax, Canada.
† Division of Engineering, Colorado School of Mines, Golden, Colorado, USA.
‡ Department of Civil Engineering, Dalhousie University, Halifax, Canada.

some margin for safety, the value of P_a may be adjusted by multiplying by a conservative factor of safety, F.

Owing to spatial variability, the failure surface is often more complicated than a simple plane, and the resulting behaviour cannot be expected to match that predicted by theory. Some work on reliability-based design of earth retaining walls has been carried out recently (e.g. Basheer & Najjar, 1996; Chalermyanont & Benson, 2004). However, these studies consider the soil to be spatially uniform: that is, each soil property is represented by a single random variable, and every point in the soil is assigned the same property value. For example, a particular realisation might have $\phi' = 32°$, which would be assumed to apply to all points in the soil mass. The assumption that the soil is spatially uniform is convenient, as most geotechnical predictive models are derived assuming spatially uniform properties (e.g. Rankine's earth pressure theory). These studies serve to help develop understanding of the underlying issues in reliability-based design of retaining walls but fail to include the effects of spatial variability. As will be seen, the failure surface can be significantly affected by spatial variability.

When spatial variability is included in the soil representation, alternative tractable solutions to the reliability issue must be found. For geotechnical problems that do not depend too strongly on extreme micro-scale soil structure (i.e. which involve some local averaging), it can be argued that the behaviour of the spatially random soil can be closely represented by a spatially uniform soil, which is assigned the 'effective' properties of the spatially random soil. The authors have been successful in the past with this effective property representation, for a variety of geotechnical problems, by defining the effective uniform soil as some sort of average of the random soil; generally the geometric average has been found to work well (e.g. Fenton & Griffiths, 2003). If the above argument holds, then it implies that the spatially random soil can be well modelled by equations such as equations (1) and (2), even though these equations are based on uniform soil properties; the problem becomes one of finding the appropriate effective soil properties.

In practice, the values of ϕ' and γ used in equations (1) and (2) are obtained through site investigation. If the investigation is thorough enough to allow spatial variability to be characterised, an effective soil property can, in principle, be determined using random field theory combined with simulation results. However, the level of site investigation required for such a characterisation is unlikely to be worth carrying out for most retaining wall designs. In the more common case, the geotechnical engineer may base the design on a single estimate of the friction angle and unit weight. In this case, the accuracy of the prediction arising from equations (1) and (2) depends very much on how well the single estimate approximates the effective value.

This paper addresses the above issues. In particular, it attempts to shed light on the following questions:

(*a*) Do sampled soil properties adequately reflect the effective properties of the entire retained soil mass?
(*b*) Does spatial variability in soil properties lead to active earth pressure effects that are significantly different from those predicted using traditional equations, such as Rankine's?

Figure 1 shows plots of what a typical retained soil might look like once the retaining wall has moved enough to mobilise the active soil behaviour for two different possible realisations. The soil's spatially random friction angle is shown using a greyscale representation, where dark areas correspond to lower friction angles. Note that although the unit weight, γ, is also spatially random, its variability is not shown on the plots; its influence on the stochastic behaviour of earth pressure was felt to be less important than that of the ϕ' field.

The wall is on the left-hand face, and the deformed mesh plots of Fig. 1 are obtained using the random finite element method (RFEM) with 8-node square elements and an elastic-perfectly plastic constitutive model (see next section for more details). The wall is gradually moved away from the soil mass until plastic failure of the soil occurs, and the deformed mesh at failure is then plotted. It is clear from these plots that the failure pattern is more complex than that found using traditional theories, such as Rankine's. Instead of a well-defined failure plane, the particular realisation shown in the upper plot of Fig. 1, for example, seems to have a failure wedge forming some distance from the wall in a region with higher friction angles. The formation of a failure surface can be viewed as the mechanism by which lateral loads stabilise to a constant value with increasing wall displacement.

Figure 1 also shows that choosing the correct location to sample the soil may be important to the accuracy of the prediction of the lateral active load. For example, in the lower plot of Fig. 1, the soil sample, taken at the midpoint of the soil regime, results in a friction angle estimate that is considerably lower than the friction angle typically seen in the failure region (recall that white elements correspond to higher friction angles). The resulting predicted lateral active load, using Rankine's theory, is about 1·5 times that predicted by the RFEM, so that a wall designed using this soil sample would be overdesigned. Quite the opposite is found for the more complex failure pattern in the upper plot of Fig. 1, where the lateral active load found via the RFEM is more than twice that predicted using Rankine's theory, and so a Rankine-based design would be unconservative. The higher RFEM load is attributed to the low friction angle material found in near proximity to the wall.

THE RANDOM FINITE ELEMENT MODEL

The soil mass is discretised into 32 eight-noded square elements in the horizontal direction by 32 elements in the vertical direction. Each element has a side length of $H/16$, giving a soil block that is $2H$ wide by $2H$ deep. (Note: length units are not used here as the results can be used with any consistent set of length and force units.) The retaining wall extends to a depth H along the left face.

The finite element earth pressure analysis uses an elastic-perfectly plastic Mohr–Coulomb constitutive model with stress redistribution achieved iteratively using an elasto-viscoplastic algorithm essentially similar to that described in the text by Smith & Griffiths (2004). The active wall considered in this study is modelled by translating the top 16 elements on the upper left side of the mesh uniformly horizontally and away from the soil. This translation is performed incrementally, and models a rigid, smooth wall with no rotation.

The initial stress conditions in the mesh prior to translation of the nodes are that the vertical stresses equal the overburden pressure, and the horizontal stresses are given by Jaky's (1944) formula in which $K_0 = 1 - \sin\phi'$. As described in the next section, the study will assume that $\tan\phi'$ is a log-normally distributed random field: hence K_0 will also be a random field (albeit fully determined by ϕ'), so that the initial stresses vary randomly down the wall face.

The boundary conditions are such that the right side of the mesh allows vertical but not horizontal movement, and the base of the mesh is fully restrained. The top and left sides of the mesh are unrestrained, with the exception of the nodes adjacent to the 'wall', which have fixed horizontal components of displacement. The vertical components of these displaced nodes are free to move down, as active conditions are mobilised. These boundary conditions have been shown to work well for simple earth pressure analysis (e.g. Griffiths, 1980).

Following incremental displacement of the nodes, the viscoplastic algorithm monitors the stresses in all the elements (at the Gauss points) and compares them with the strength of the element based on Mohr–Coulomb's failure criterion. If the failure criterion is not violated, the element is assumed to remain elastic; however, if the criterion is violated, stress redistribution is initiated by the viscoplastic algorithm. The process is inherently iterative, and convergence is achieved when all stresses within the mesh satisfy the failure criterion within quite tight tolerances.

At convergence following each increment of displacement, the mobilised active reaction force on the wall is computed by integrating the stresses in the elements attached to the displaced nodes. The finite element analysis is terminated when the incremental displacements have resulted in the active reaction force reaching its minimum limiting value.

The cohesionless soil being studied here has two properties of primary interest to the active earth pressure problem: these are the friction angle, $\phi'(\underset{\sim}{x})$, and unit weight, $\gamma(\underset{\sim}{x})$, where $\underset{\sim}{x}$ is the spatial position. Both are considered to be spatially random fields. The finite element model used in this study also includes the soil's dilation angle, taken to be zero, Poisson's ratio, taken to be 0·3, and Young's modulus, taken to be 1×10^5. These three properties are assumed to be spatially constant; this does not introduce significant error, as these properties play only a minor role in the development of active earth pressures.

The two properties that are considered to be spatially random, ϕ' and γ, are characterised by their means, their standard deviations, and their correlation lengths (which are measures of the degree of spatial correlation). The unit weight is assumed to have a log-normal distribution, primarily because of its simple relationship with the normal distribution, which is fully specified by the first two moments, and because it is non-negative. The friction angle, ϕ', is generally bounded, which means that its distribution is a complicated function with at least four parameters (Fenton & Griffiths, 2003). However, $\tan\phi'$ varies between 0 and infinity as ϕ' varies between 0° and 90°. Thus a possible distribution for $\tan\phi'$ is also the log-normal. This distribution will be assumed in this paper: that is, the friction angle field will be represented by the log-normally distributed $\tan\phi'$ field.

The spatial correlation structures of both fields will be assumed to be the same. This is not only for simplicity, as it can be argued that the spatial correlation of a soil is governed largely by the spatial variability in a soil's source materials, weathering patterns, stress and formation history etc. That is, the material source, weathering, stress history etc. forming a soil at a point will be similar to that at a closely neighbouring point, so one would expect that all the soil's properties will vary similarly between the two points (aside from deviations arising from differing non-linear property response to current conditions).

With this argument in mind, the spatial correlation function for the $\ln(\gamma)$ and $\ln(\tan\phi')$ fields, both normally distributed, is assumed to be Markovian:

$$\rho(\tau) = \exp\left\{\frac{-2|\underset{\sim}{\tau}|}{\theta}\right\} \tag{3}$$

where θ is the correlation length beyond which two points in the field are largely uncorrelated, $\underset{\sim}{\tau}$ is the vector between the two points, and $|\underset{\sim}{\tau}|$ is its absolute length.

In this study, the two random fields, γ and $\tan\phi'$, are first assumed to be independent. Thus two independent standard normal random fields, $G_1(\underset{\sim}{x})$ and $G_2(\underset{\sim}{x})$, are simulated by the local average subdivision (LAS) method (Fenton & Vanmarcke, 1990), using the correlation structure given by equation (3). These fields are then transformed to the target fields through the relationships

$$\gamma(\underset{\sim}{x}) = \exp\{\mu_{\ln\gamma} + \sigma_{\ln\gamma} G_1(\underset{\sim}{x})\} \tag{4a}$$

$$\tan\phi'(\underset{\sim}{x}) = \exp\{\mu_{\ln\tan\phi'} + \sigma_{\ln\tan\phi'} G_2(\underset{\sim}{x})\} \tag{4b}$$

where μ and σ are the mean and standard deviation of the subscripted variable, obtained using the following transformations:

$$\sigma^2_{\ln\gamma} = \ln(1 + V^2_\gamma) \tag{5a}$$

$$\mu_{\ln\gamma} = \ln(\mu_\gamma) - \tfrac{1}{2}\sigma^2_{\ln\gamma} \tag{5b}$$

and $V_\gamma = \sigma_\gamma/\mu_\gamma$ is the coefficient of variation of γ. A similar transformation can be applied for the mean and variance of $\tan\phi'$ by replacing γ with $\tan\phi'$ in the subscripts of equation (5).

As the friction angle, ϕ', and the unit weight, γ, generally have a reasonably strong positive correlation, a second case will be considered in this study where the two fields are significantly correlated: specifically, a correlation coefficient of $\rho = 0{\cdot}8$ will be assumed to act between $\ln(\gamma)$ and $\ln(\tan\phi')$ at each point in the soil. Thus, when the friction angle is large, the unit weight will also tend to be large, within their respective distributions. The correlation between the fields is implemented using the covariance matrix decomposition method (e.g. Fenton, 1994).

Once realisations of the soil have been produced using LAS and the above transformations, the properties can be mapped to the elements and the soil mass analysed by the finite element method. See Fig. 1 for two examples. Repeating this analysis over a sequence of realisations (Monte Carlo simulation) yields a sequence of computed responses, allowing the distribution of the response to be estimated.

ACTIVE EARTH PRESSURE DESIGN RELIABILITY

As mentioned in the introduction, the design of a retaining wall involves two steps: (a) estimating the pertinent soil properties, and (b) predicting the lateral load through, for example, equation (2). The reliability of the resulting design depends on the relationship between the predicted and actual lateral loads. Disregarding variability on the resistance side and assuming that the design wall resistance, R, satisfies

$$R = FP_a \tag{6}$$

where F is a factor of safety and P_a is the predicted active lateral earth load (equation (2)), then the wall will survive if the true active lateral load, P_t, is less than FP_a. The true active lateral load will inevitably differ from that predicted because of errors in the estimation of the soil properties and because of the spatial variability present in a true soil, which is not accounted for by classical theories, such as equations (1) and (2). The probability of failure of the retaining system will be defined as the probability that the true lateral load, P_t, exceeds the factored resistance:

$$p_f = P[P_t > R] = P[P_t > FP_a] \tag{7}$$

This is the theoretical definition of the failure probability, p_f. In the following section, the estimate of this failure probability, $\hat{p}_f$, will be obtained by Monte Carlo simulation. The 'true' (random) lateral load, P_t, will be assumed in this study to be closely approximated by the load computed in the

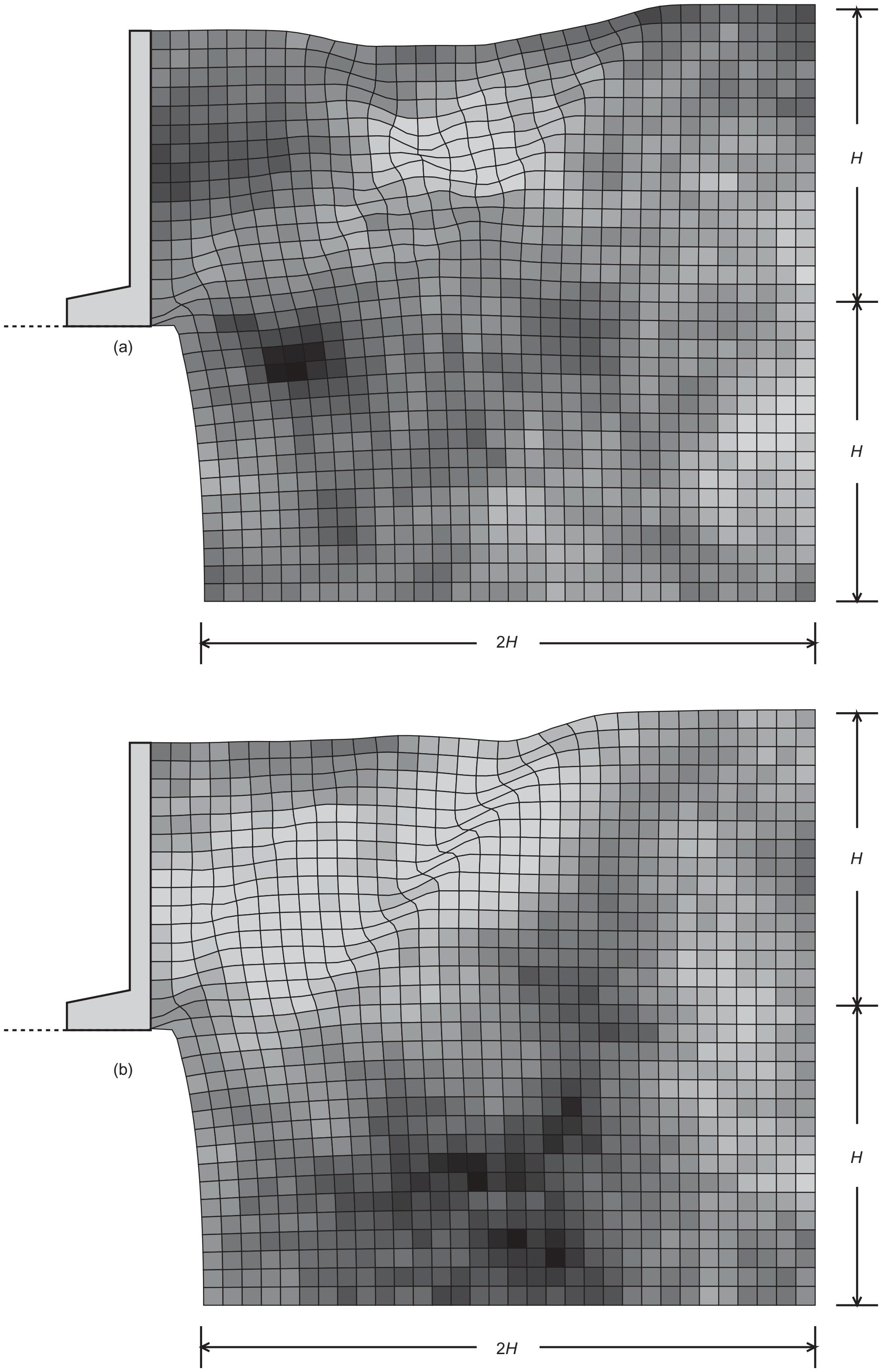

Fig. 1. Active earth displacements for two different possible soil friction angle field realisations (both with $\theta/H = 1$ and $\sigma/\mu = 0{\cdot}3$)

finite element analysis of each soil realisation. That is, it is assumed that the finite element analysis, which accounts for spatial variability, will produce a realistic assessment of the actual lateral active soil load for a given realisation of soil properties.

The predicted lateral load, P_a, depends on an estimate of the soil properties. In this paper, the soil properties γ and $\tan\phi'$ will be estimated using only a single 'virtual sample' taken at a distance H in from the base of the retaining wall and a distance H down from the soil surface. The phrase 'virtual sample' means that the properties are sampled from the random field realisations assigned to the finite element mesh. Specifically, virtual sampling means that for $\underset{\sim}{x}_s$ being the coordinates of the sample point, the sampled soil properties $\hat{\gamma}$ and $\hat{\phi}'$ are obtained from each random field realisation as

$$\hat{\gamma} = \gamma(\underset{\sim}{x}_s) \tag{8a}$$

$$\hat{\phi}' = \tan^{-1}\{\tan[\phi'(\underset{\sim}{x}_s)]\} \tag{8b}$$

Armed with these sample properties, the predicted lateral load becomes

$$P_a = \tfrac{1}{2}\hat{\gamma}H^2\tan^2\left(45 - \frac{\hat{\phi}'}{2}\right) \tag{9}$$

No attempt is made to incorporate measurement error. The goal of this study is to assess the design risk arising from the spatial variability of the soil, and not from other sources of variability.

Table 1 lists the statistical parameters varied in this study. The coefficient of variation, $V = \sigma/\mu$, is changed for both the unit weight, γ, and the friction, $\tan\phi'$, fields identically. That is, when the coefficient of variation of the unit weight field is 0·2, the coefficient of variation of the $\tan\phi'$ field is also 0·2, and so on. For each parameter set considered in Table 1, the factor of safety, F, is varied from 1·5 to 3·0. This range is somewhat wider than the range of 1·5 to 2·0 recommended, for example, by the Canadian Foundation Engineering Manual (Canadian Geotechnical Society, 1992) for retaining wall systems.

The correlation length, θ, which is normalised in Table 1 by expressing it as a fraction of the wall height, θ/H, governs the degree of spatial variability. When θ/H is small, the random field is typically rough in appearance: points in the field are more independent. Conversely, when θ/H is large, the field is more strongly correlated, so that it appears smoother with less variability in each realisation. A large scale of fluctuation has two implications: first, the soil properties estimated by sampling the field at a single location will be more representative of the overall soil mass; and, second, the reduced spatial variability means that the soil will behave more like that predicted by traditional theory. Thus, for larger correlation lengths, fewer 'failures' are expected (where the actual lateral limit load exceeds the factored prediction), and the factor of safety can be reduced. For intermediate correlation lengths, however, the soil properties measured at one location may be quite different from those actually present at other locations. Thus, for intermediate correlation lengths, more 'failures' are expected. When the correlation length becomes extremely small—much smaller than the soil property sample size—local averaging effects begin to take over, and both the sample and overall soil mass return to being an effectively uniform soil (with properties approaching the median), accurately predicted by traditional theory using the sample estimate.

Following this reasoning, the maximum probability of failure of the design is expected to occur when the correlation length is some intermediate value. Evidence supporting this argument is found in the next section.

MONTE CARLO RESULTS

Both plots of Fig. 1 indicate that it is the high friction angle regions that attract the failure surface in the active case. Although this is not always the case for all realisations, it tends to be the most common behaviour. Such a counter-intuitive observation seems to be due largely to the interaction between the initial horizontal stress distribution, as dictated by the $K_0 = 1 - \sin\phi'$ random field, and the friction angle field.

To explain this behaviour, it is instructive to consider the Mohr's circles corresponding to $K_0 = 1 - \sin\phi'$ (at rest, initial, conditions) and $K_a = (1 - \sin\phi')/(1 + \sin\phi')$ (active failure conditions). As ϕ' increases from 0°, the distance between the initial and failure circles increases, reaching a maximum when $\phi' = \tan^{-1}(0{\cdot}5\sqrt{2}\sqrt{\sqrt{2}-1}) = 24{\cdot}47°$. Beyond this point, the distance between the initial and failure circles decreases with increasing ϕ'. As the average drained friction angle used in this study is 30° (to first order), the majority of realisations of ϕ' are in this region of decreasing distance between circles. This supports the observation that, under these conditions, the higher friction angle regions tend to reach active failure first. One point that comes out of this is that failure is always attracted to the weakest zones, even if those weakest zones happen to have a higher friction angle. In this sense the greyscale shown in Fig. 1 is telling only part of the story; it is really the shear strength ($\sigma'\tan\phi'$) that is important.

The attraction of the failure surface to the high friction angle regions is due to the fact that the initial conditions vary with ϕ' according to Jaky's formula in this study. In a side investigation, it was found that, if the value of K_0 is held fixed, then the failure surface does pass through the lower friction angle regions. Fig. 2 shows the effect that K_0 has on the location of the failure surface. In Fig. 2(a) K_0 is held spatially constant at 0·5, and in this case the failure surface clearly migrates towards the low friction angle regions. In Fig. 2(b) K_0 is set equal to $1 - \sin\phi'$, as in the rest of the paper, and the failure surface clearly prefers the high friction angle regions. The authors also investigated the effect of spatially variable as against spatially constant unit weight and found that this had little effect on the failure surface location, at least for the levels of variability considered here. The location of the failure surface seems to be governed primarily by the nature of K_0 (given random ϕ').

The migration of the failure surface through the weakest path means that, in general, the lateral wall load will be different from that predicted by a model based on uniform soil properties, such as Rankine's theory. Fig. 3 shows the estimated probability of failure, $\hat{p}_f$, that the actual lateral active load will exceed the factored predicted design load (see equation (7)) for a moderate correlation length ($\theta/H = 1$) and for various coefficients of variation in the friction angle and unit weight. The estimates are obtained by counting the number of failures encountered in the simulation and dividing by the total number of realisations considered ($n = 1000$). In that this is an estimate of a proportion, its standard error (one standard deviation) is $\sqrt{p_f(1 - p_f)/n}$, which is about 1% when $p_f = 20\%$ and about 0·3% when $p_f = 1\%$. The figure shows two cases: (a) where the friction angle and unit weight fields are independent; and (b) where there is a strong correlation between the two fields.

As expected, the probability of failure increases as the soil becomes increasingly variable. Fig. 3 can be used to determine a required factor of safety corresponding to a target probability of failure. For example, if the fields are assumed to be independent (Fig. 3(a)), with $V = 0{\cdot}2$, and the soil properties are sampled as in this study, then a required factor of safety of about $F = 2$ is appropriate for a target probability of failure of 5%. The required factor of safety increases to 3 or more when $V \geqslant 0{\cdot}3$. Recalling that only one sample is used in this study to characterise the soil, and that the sample is well outside the expected failure zone

Table 1. Parameters varied in the study while holding the retained soil dimension H, and soil properties $\mu_{\tan\phi'} = \tan 30°$, $\mu_\gamma = 20$, $E = 1 \times 10^5$ and $\nu = 0{\cdot}3$ constant. For each parameter set, 1000 realisations were run.

Parameter	Values considered
σ/μ	0·02, 0·05, 0·1, 0·2, 0·3, 0·5
θ/H	0·1, 0·2, 0·5, 1·0, 2·0, 5·0
ρ	0·0, 0·8

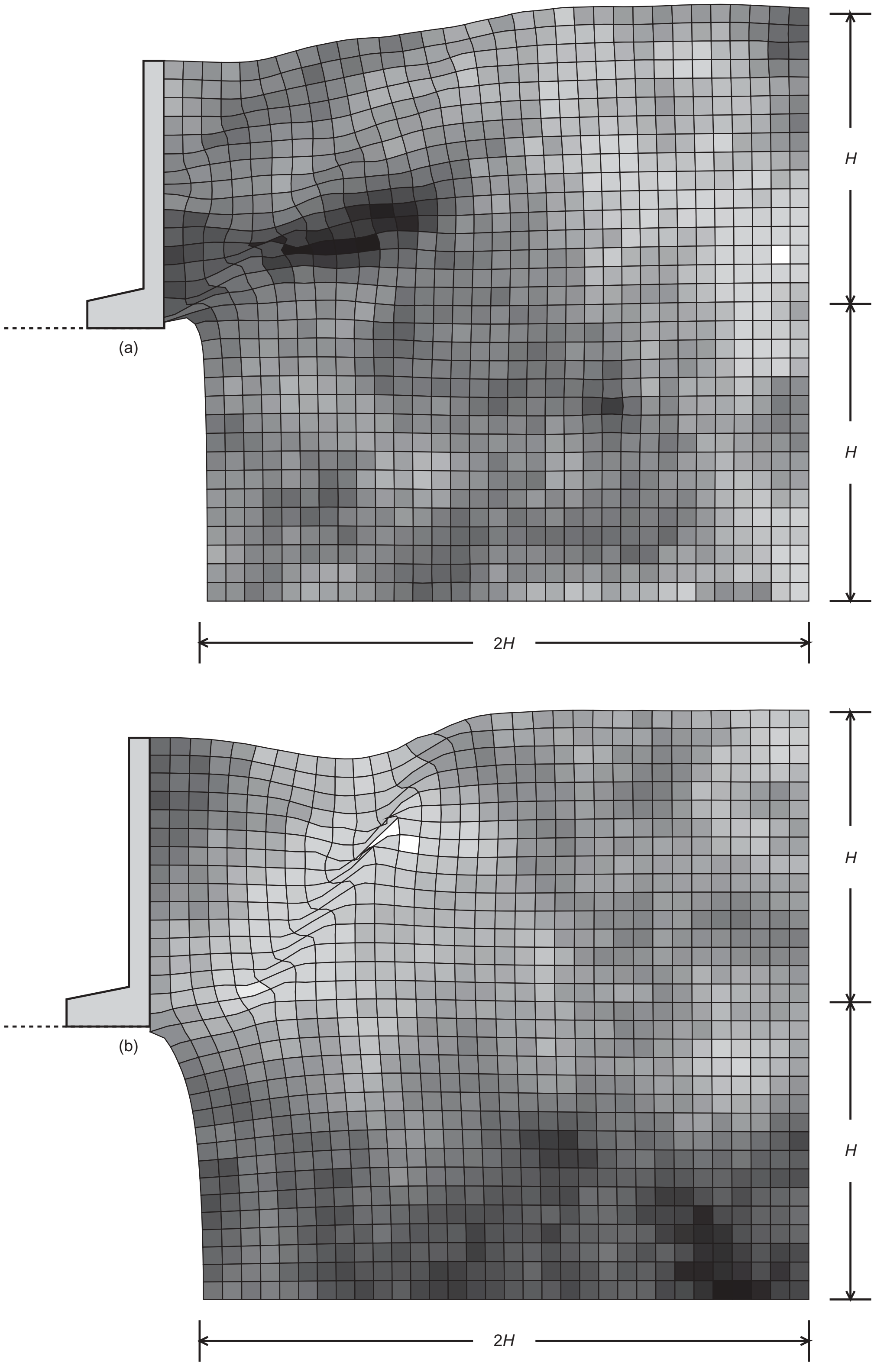

Fig. 2. Active earth displacements for two different possible soil friction angle field realisations (both with $\theta/H = 1$ and $\sigma/\mu = 0{\cdot}3$): (a) K_0 held spatially constant at 0·5; (b) $K_0 = 1 - \sin\phi'$ is a spatially random field derived from ϕ'

(albeit without any measurement error), the required factor of safety may be reduced if more samples are taken, or if the sample is taken closer to the wall, resulting in a more accurate characterisation of the soil.

Figure 3(b) shows the estimated probability of failure for the same conditions as in Fig. 3(a), except that now the friction angle and unit weight fields are strongly correlated ($\rho = 0{\cdot}8$). The main effects of introducing correlation between the two fields are: (a) slightly reducing the average wall reaction; and (b) significantly reducing the wall reaction variance (correlation between 'input' parameters tends to reduce variance in the 'output'). These two effects lead to a reduction in failure probability, which leads in turn to a reduction in the required factor of safety for the same target

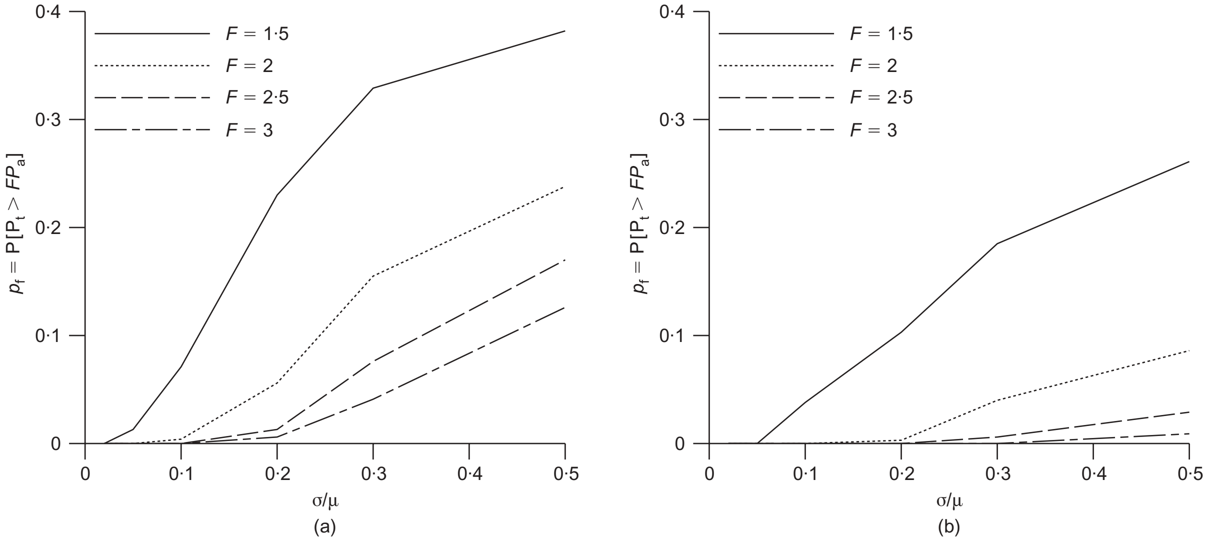

Fig. 3. Estimated probability that actual load exceeds design load, $\hat{p}_f$, for $\theta/H = 1$: (a) ϕ' and γ fields are independent ($\rho = 0$); (b) the two fields are strongly correlated ($\rho = 0{\cdot}8$)

failure probability. For example, the required factor of safety in the case of strongly correlated fields with $V \geqslant 0{\cdot}3$ is only $F \geqslant 2$ for a probability of failure of 5%.

Figure 4 shows the estimated probability of failure, $\hat{p}_f$, for a coefficient of variation of 20% against the correlation length, θ/H, for the two cases of (a) independence between the friction angle and unit weight fields, and (b) strong correlation between the fields. Notice that, for the correlated fields of Fig. 4(b), the probability of failure is negligible for all $F \geqslant 2$ when the coefficient of variation is 20%.

Of interest in Fig. 4 is the fact that there is a 'worst case' correlation length, where the probability of failure reaches a maximum. A similar worst case is seen in all of the soil coefficients of variation considered. This worst-case correlation length is typically of the order of the depth of the wall ($\theta = 0{\cdot}5H$ to $\theta = H$). The importance of this observation is that this worst-case correlation length can be conservatively used for reliability analyses in the absence of improved information. As the correlation length is quite difficult to estimate in practice, requiring substantial data, a methodology that does not require its estimation is preferable.

CONCLUSIONS

On the basis of this simulation study, the following observations can be made:

(*a*) The behaviour of a spatially variable soil mass is considerably more complex than suggested by the simple models of Rankine and Coulomb. The traditional approach to compensating for this model error is to appropriately factor the lateral load predicted by the model.

(*b*) The failure mode of the soil in the active case suggests that the failure surface is controlled by high friction angle regions when K_0 is defined according to Jaky's

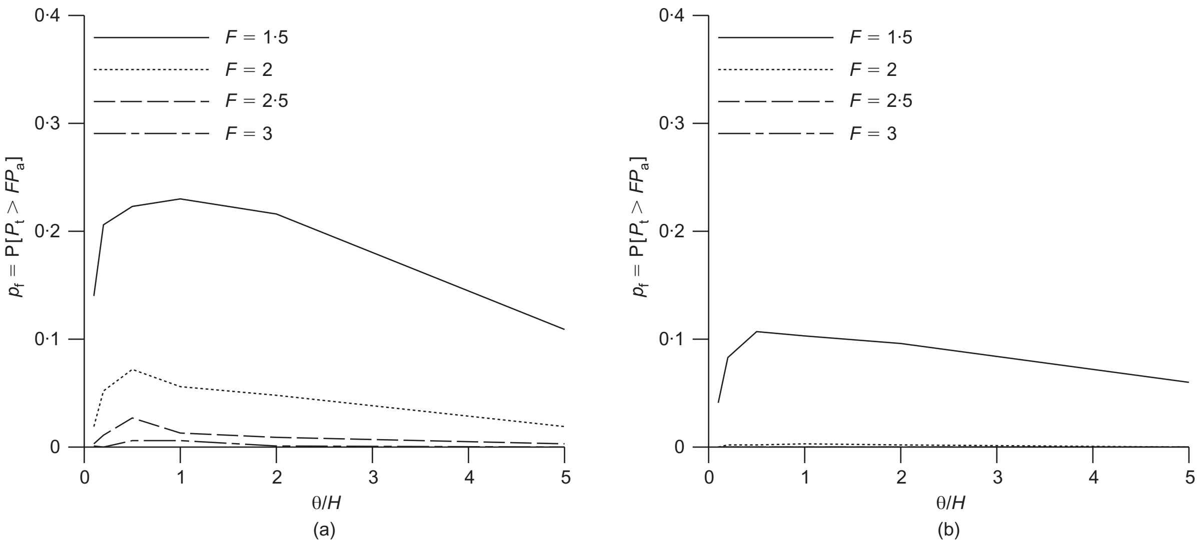

Fig. 4. Estimated probability that actual load exceeds design load, $\hat{p}_f$, for $\sigma/\mu = 0{\cdot}2$: (a) ϕ' and γ fields are independent ($\rho = 0$); (b) the two fields are strongly correlated ($\rho = 0{\cdot}8$)

formula (and is thus spatially variable). When K_0 is held spatially constant, the failure surface tends to pass preferentially through the low friction angle regions.

(*c*) Taking the friction angle and unit weight fields to be independent is conservative, in that it leads to higher estimated probabilities of failure.

(*d*) In the case when the friction angle and unit weight fields are taken to be independent, and when the soil is sampled at a single point at a moderate distance from the wall, the probabilities of failure are quite high, and a factor of safety of about 2·0–3·0 is required to maintain a reasonable reliability (95%), unless it is known that the coefficient of variation for the soil is less than about 20%. Since, for larger coefficients of variation, the required factors of safety are above those recommended by, say, the Canadian Foundation Engineering Manual (CFEM), the importance of a more than minimal site investigation is highlighted.

(*e*) Assuming a strong correlation between the friction angle and unit weight fields leads to factors of safety that are more in line with those recommended by CFEM. However, further research is required to determine whether (and under what conditions) this strong correlation should be depended upon in a design.

(*f*) As has been found for a number of different classical geotechnical problems (e.g. differential settlement and bearing capacity), a worst-case scale of fluctuation exists for the active earth pressure problem, which is of the order of the retaining wall height. The important implication of this observation is that the scale of fluctuation need not be estimated; the worst-case scale can be used to yield a conservative design at a target reliability. This is a practical advantage, because the scale of fluctuation is generally difficult and expensive to estimate accurately, requiring a large number of samples.

In summary, there is much that still needs to be investigated to fully understand the probabilistic active behaviour of retained soils. In particular, the effect of sampling intensity on design reliability, and the type of sample average best suited to represent the effective soil property, are two areas that must be investigated further, using this study as a basis, before a formal reliability-based design code can be developed.

ACKNOWLEDGEMENTS

The authors would like to thank the National Sciences and Engineering Research Council of Canada, under Discovery Grant RGPIN0105445, and the National Science Foundation of the United States of America, under Grant CMS-0408150, for their essential support of this research. Any opinions, findings, conclusions or recommendations are those of the authors, and do not necessarily reflect the views of the aforementioned organisations.

NOTATION

E	Young's modulus
F	factor of safety
$G(\underset{\sim}{x})$	standard normal (Gaussian) random field
H	depth of retaining wall
K_a	active earth pressure coefficient
K_0	coefficient of earth pressure at rest
n	number of realisations
p_f	probability of failure, i.e. $P[P_t > FP_a]$
P_a	active lateral load on retaining wall predicted by Rankine
P_t	true lateral load on retaining wall (approximated by RFEM)
R	retaining wall design resistance, FP_a
V	coefficient of variation, σ/μ
$\underset{\sim}{x}$	spatial coordinate or position
γ	unit weight
$\hat{\gamma}$	estimated unit weight
θ	correlation length
μ	random field mean
μ_γ	mean unit weight
$\mu_{\tan\phi'}$	mean of tangent of drained friction angle
$\mu_{\ln\gamma}$	mean of logarithm of unit weight
$\mu_{\ln\tan\phi'}$	mean of logarithm of tangent of drained friction angle
ν	Poisson's ratio
ρ	point-wise correlation between $\ln\gamma$ and $\ln(\tan\phi')$ random fields
σ	random field standard deviation
$\sigma_{\ln\gamma}$	standard deviation of logarithm of unit weight
$\sigma_{\ln\tan\phi'}$	standard deviation of the logarithm of the tangent of the drained friction angle
σ'	effective stress
$\underset{\sim}{\tau}$	vector between two points in a random field
ϕ'	drained internal friction angle
$\hat{\phi}'$	estimated drained internal friction angle

REFERENCES

Basheer, I. A. & Najjar, Y. M. (1996). Reliability-based design of reinforced earth retaining walls. *Transportation Research Record*, No. 1526, 64–78.

Canadian Geotechnical Society (1992). *Canadian foundation engineering manual*. Montreal: Canadian Geotechnical Society.

Chalermyanont, T. & Benson, C. H. (2004). Reliability-based design for internal stability of mechanically stabilized earth walls. *ASCE J. Geotech. Geoenviron. Engng* **130**, No. 2, 163–173.

Fenton, G. A. (1994). Error evaluation of three random field generators. *ASCE J. Engng Mech.* **120**, No. 12, 2478–2497.

Fenton, G. A. & Griffiths, D. V. (2003). Bearing capacity of spatially random c–ϕ soils. *Can. Geotech. J.* **40**, No. 1, 54–65.

Fenton, G. A. & Vanmarcke, E. H. (1990). Simulation of random fields via local average subdivision. *ASCE J. Engng Mech.* **116**, No. 8, 1733–1749.

Griffiths, D. V. (1980). Finite element analyses of walls, footings and slopes. *Proceedings of a symposium on computer applications to geotechnical problems in highway engineering*, Cambridge, UK, pp. 122–146.

Jaky, J. (1944). The coefficient of earth pressure at rest. *J. Soc. Hung. Archit. Engrs*, 355–358.

Smith, I. M. & Griffiths, D. V. (2004). *Programming the finite element method*, 4th edn. New York: John Wiley & Sons.